Proceedings of the Eleventh (2014) Pacific/Asia Offshore Mechanics Symposium **www.isope.org**
Shanghai, China, October 12-16, 2014

ISBN 978–1 880653 90-6: ISSN 1946-004X

Numerical Computation of Aerodynamic Performances of NREL Offshore 5-MW Baseline Wind Turbine

*Wenchao Zhao, Ping Cheng, Decheng Wan**
State Key Laboratory of Ocean Engineering, School of Naval Architecture, Ocean and Civil Engineering,
Shanghai Jiao Tong University, Shanghai, China
*Corresponding author

ABSTRACT

With the development of the offshore wind turbine technology, the offshore wind turbine is going to deeper waters, and the scale of the offshore wind turbine is becoming larger, in which case the numerical computation of aerodynamic performances of large-scale floating offshore wind turbines is becoming more and more important. In this paper, NREL offshore 5-MW baseline wind turbine of the Phase II of the Offshore international Code Comparison Collaboration Continuation (OC4) project has had been selected as the object as its detailed data and widely concern, the multiple reference frame(MRF) method based on open source code OpenFOAM is used, the aerodynamic performance of the 5-MW baseline wind turbine under different wind speeds without considering the impact of the floating structure is simulated, and the rotor thrust, torque, pressure coefficient and wake vortex aerodynamic data and flow field information were obtained in detail.

KEY WORDS: offshore wind turbine; aerodynamic performance; OC4; MRF; OpenFOAM.

INTRODUCTION

As the energy crisis and environment crisis emerge, more and more countries strive to search for new energy. Among all kinds of new energy, wind energy, which is clean, renewable and widely available, stands out because of its promising commercial prospect and the mature technology. Offshore wind turbines have many special and strong advantages over those wind turbines installed on land, so the offshore wind turbines become more and more attractive. At present, most offshore wind turbines are fixed-type, which are installed in shallow water. With the development of the offshore installation construction technology and the formation of commercial scale effect, the floating offshore wind turbines with higher capacity will be an key trend of the future offshore wind.

The vision for large-scale offshore floating wind turbines was introduced by Professor William E. Heronemus (1972), but it was not until the mid 1990's, after the commercial wind industry was well established, that the topic was taken up again by the mainstream research community(Musial et al, 2007).

The aerodynamic performance analysis of offshore wind turbines is the foundation of offshore wind turbines design and research, and also is one of the key technologies. The aerodynamic performance of the blades directly determines the capacity of the wind turbine. As the higher capacity is required, which means larger scale offshore wind turbine at the same time, the aerodynamic performance of the blades even plays a more important role in the design. So the numerical simulation of the aerodynamic performance of the offshore wind turbines is an essential process.

At present, there are basically three main method for the aerodynamic performance simulation of the wind turbines: the Blade Element Momentum theory (BEM); the Generalized Dynamic Wake model (GDW); and the Computational Fluid Dynamics (CFD).

The Blade element momentum (BEM) theory is one of the oldest and most commonly used methods for calculating induced velocities on wind turbine blades, which was first proposed by the pioneering propeller work of Rankine and Froude in the late 19th century (Moriaty et al, 2005).The advantage of the BEM theory is that each blade element is modeled as a two-dimensional airfoil, which means less computational costs. But the BEM theory has a great dependence on the airfoil experiment data, which will directly affect the accuracy of the Aerodynamic load calculating.

The Generalized Dynamic Wake method (GDW), also known as the acceleration potential method, was originally developed for the helicopter industry. The GDW method is based on a potential flow solution to Laplace's equation. An advantage of this method is that it allows for a more general distribution of pressure across a rotor plane than BEM theory. This method assumes the rotor plane of the wind turbine as a flat disc, so it lacks of accuracy when simulate the aerodynamic performance of wind turbine with big cone angle and the effects of large blade deformation.

In the Computational Fluid Dynamics(CFD) method, based on the Navier-Stokes equation, the flow field around the wind turbine blades is divided into computing grids, and the Navier-Stokes equation will be discretized on each grid node, which generates a lot of nonlinear coupled equations and takes a great deal of computational resources and time. But using the Computational Fluid Dynamics (CFD) method, we can get more detailed information in the flow field. So with the rapid development of computing technology, the CFD method will gradually

become a powerful tool of flow field simulation and performance prediction for wind turbines. In this paper, the CFD method was chosen to simulate the aerodynamic performance of offshore floating turbines.

As the Navier-Stocks equation itself is not closed, a appropriate turbulence model is needed. Currently, the widely used turbulence model for 2-D aerodynamic performance simulation of the wind turbine is the k-ω SST model, which was proposed by Menter (1993) . The SST k-ω turbulence model is a two-equation eddy-viscosity model which combines the advantages of two turbulence models: the k-ω model and the k-ε model. Sørensen et al (2002) simulated the aerodynamic performance of a single blade of the wind turbine Phase VI with the SST k-ω turbulence model using the incompressible RANS solver EllipSys3D based on the multi-block finite volume. In the research, the torque from the simulation has a 20% deviation with that from the experiments when the wind speed was over 13 m/s, while the pressure distribution and some other results matched well with the experimental results. Shur et al (1999), Strelets (2001), Johansen et al (2002) and other scholars have tried the Detached Eddy Simulation (DES) method for aerodynamic performance simulation of the two-dimensional airfoil of the wind turbine. Due to the DES method needs more detailed meshing, so its computational cost is quite striking, which becomes an obstacle to its further application. Li et al (2012) simulates the National Renewable Energy Laboratory (NREL) phase VI wind turbine using dynamic overset grid technology. In the simulation the unsteady Reynolds-Averaged Navier–Stokes (RANS) and Detached Eddy Simulation (DES) turbulence models were used, and both showed little difference in the averaged forces and moments. With the rapid development of computing technology, the grid size that the numerical model can deal with is also rising. Fleig et al (2004) calculated the far-field broadband noise caused by a rotating blade of the MELIII wind turbine using compressible Large-Eddy Simulation (LES) method with about 300 million grid points. So with the development of the CFD technology, the CFD method will be an key method for the simulation of the aerodynamic performance of wind turbines in the future.

OpenFOAM, short for Open Source Field Operation and Manipulation, is the open source CFD software package. Because of its flexibility, open source, and parallel nature combined with its availability at no cost, OpenFOAM becomes more and more popular. And it's also an excellent choice in the study of wind turbines (Stovall, 2010; Churchfield et al, 2012).

SIMULATION METHOD

The Multi Reference Framework (MRF) method is one of the most common methods in dealing with grid relative rotating or moving. In transient coordinate reference frame, the rotation motion of wind turbine blade is transient. But when we put the rotating wind turbine blade into a rotating coordinate reference frame, the rotation motion of blade can be converted to static calculation problem. The simulation domain will be divided into different subdomains according to the relative motion of the grid, then the control equations will be established based on different reference frames in every subdomain. The information of the whole flow field exchanges by the mutual conversion between the relative velocity and absolute velocity. In addition, the numerical simulation of multiple wind turbines, even of the whole wind farm can be done with the Multi Reference Framework (MRF) method, which is a significant advantage of the method.

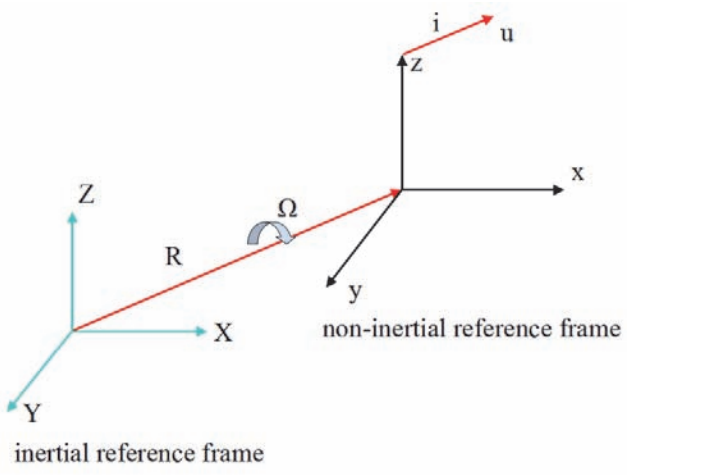

Fig 1. Relationship between inertial reference frame and non-inertial reference frame (r represents the position vector; R the velocity vector; Ω the rotating angular velocity vector)

When the Multi MRF method is used, the coordinate system will rotate with the rotating blade, in which case the Navier - Stokes equations used in the inertial reference frame doesn't work. So the relationship between inertial reference frame and non-inertial reference frame should be built up (Fig.1).

Two types of forces related to the rotation will be added in the Navier - Stokes equations: the Coriolis force $\rho[2\Omega \times u]$ and the centrifugal force $\rho[\Omega \times \Omega \times r]$.

So the Navier - Stokes equations is given as:

$$\rho \frac{Du}{Dt} = -\nabla p + \mu \nabla^2 u - \rho[2\Omega \times u + \Omega \times \Omega \times r] \qquad (1)$$

In which, r indicates the position vector of the rotating coordinate system, Ω the rotating Angular velocity of the non inertial reference frame around the inertial reference frame. The solver MRFSimpleFOAM in OpenFOAM applies the MRF method to solving the incompressible viscous fluid. And in this paper, the MRFSimpleFOAM was used.

SIMULATION MODEL

NREL Offshore 5-MW Baseline Wind Turbine

In this paper, the NREL (National Renewable Energy Laboratory) offshore 5-MW baseline wind turbine (Jonkman et al, 2009) was chosen as the simulation model.

To support concept studies aimed at assessing offshore wind technology, the "NREL offshore 5-MW baseline wind turbine", a representative utility-scale multi-megawatt turbine, was developed. This wind turbine is a conventional three-bladed upwind variable-speed variable blade-pitch-to-feather-controlled turbine (Jonkman et al, 2009). As Jonkman(2007) said: "The NREL offshore 5-MW baseline wind turbine model has been, and will continue to be, used as a reference by research teams throughout the world to standardize baseline offshore wind turbine specifications and to quantify the benefits of advanced land- and sea-based wind energy technologies".

The properties of the NREL offshore 5-MW baseline wind turbine are listed in Table.1, and the structural properties of the blade are listed in Table.2 (Jonkman, 2009).

Table 1. Summary of the NREL 5MW Baseline Wind Turbine properties

Rating	5MW
Wind Regime	IEC 61400-3 (Offshore) Class 1B / Class 6 winds
Rotor Orientation	Upwind
Control	Variable Speed, Collective Pitch
Rotor Diameter / Hub Diameter	126m / 3m
Hub Height	90m
Maximum Rotor / Generator Speed	12.1rpm / 1,173.7rpm
Maximum Tip Speed	80m/s
Overhang / Shaft Tilt / Precone	5m / 5º / 2.5º

Table 2. Summary of the Blade Structural Properties

Length (w.r.t. Root Along Preconed Axis)	61.5m
Mass Scaling Factor	4.536%
Overall (Integrated) Mass	17,740 kg
Second Mass Moment of Inertia (w.r.t. Root)	11,776,047 kg-m^2
First Mass Moment of Inertia (w.r.t. Root)	363,231 kg-m
c.g. Location (w.r.t. Root Along Preconed Axis)	20.475m
Structural Damping Ratio (All Modes)	0.477465%

Simulation Domain and Grid Generation

Acordding to the structural properties listed in Table.1 and Table.2, the simulation domain was generated, which is shown in Fig.2 (a). The simulation domain is a cylinder with a diameter of 250m (about four times of the blade radius). The length of the cylinder is 240m, and the model is set 60m(about one blade radius) to the inlet face and 180m(about three times of the blade radius) to the outlet boundary(shown in Fig.2(b)and (c)). The rotating region inside the simulation domain is also a cylinder with a diameter of 90m and a length of 125m which is started from 5m before the blades and ended at 120m behind the blades(shown in Fig.2(b)and (c)).

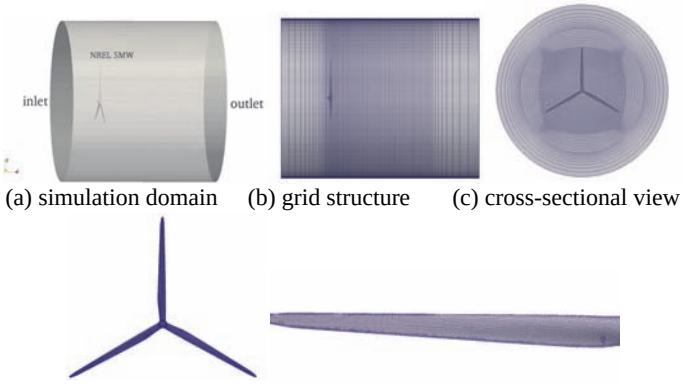

(a) simulation domain (b) grid structure (c) cross-sectional view

(d) grid structure on blades (e) enlarged view of grid structure

Fig 2. Grid Structure of the Simulation Domain and the Simulation Model

The grid for simulation was generated in two steps: first generated the backgroud grid in the ANSYS ICEM-CFD, and then refined the mesh around the blades with snappyHexMesh, supplied with OpenFOAM(shown in Fig.2(b-e)).

NUMERICAL RESULTS

In the simulation by the NREL(the National Renewable Energy Laboratory) (Jonkman, 2009), a number of FAST simulations at many fixed wind speeds in the range of 3m/s to 25m/s were run. So in this paper, the aerodynamic performance of the wind turbine under several different fixed wind speeds in the range of 3m/s to 25m/s (Jonkman, 2009) were simulated, and the rotor thrust, torque, pressure coefficient and wake vortex aerodynamic data and flow field information were obtained in detail. In the seven wind speeds, as listed in Table.3 (Jonkman, 2009), four of them are under the rated wind speed range (11.4m/s) (case 1~case 4 in Table.3), while the other three are over the rated wind speed. Usually, when the simulation wind speed is over the rated one, a pitch angle will be set on the blades (case 5~case 7 in Table.3), because the NREL 5MW baseline wind turbine incorporates a control system which has a variable-speed generator torque controller and a collective blade pitch controller. While in this paper we added three simulation cases (case 8~case 10 in Table.3), in which no pitch angle was set even when the simulation wind speed is over the rated wind speed, to see the aerodynamic performance of the turbine at over rated speed.

Table 3. Simulation Cases

Case	Wind Speed (m/s)	Rotation Speed (r/min)	Pitch Angle(deg)
1	5	7.39	0
2	8	9.16	0
3	9	10.3	0
4	11	11.89	0
5	15	12.1	10.45
6	20	12.1	17.47
7	25	12.1	23.47
8	15	12.1	0
9	20	12.1	0
10	25	12.1	0

Rotor Thrust and Torque

Table 4. Rotor Thrust and Torque

Case	Wind Speed (m/s)	Thrust ($\times 10^5$N)	Torque($\times 10^6$N*m)
1	5	2.44	0.670
2	8	4.718	2.117
3	9	5.977	2.682
4	11	8.232	4.064
5	15	5.244	4.497
6	20	4.190	4.744
7	25	3.533	4.57
8	15	10.27	7.026
9	20	11.29	9.430
10	25	12.14	10.53

As mentioned above, the aerodynamic performance of the wind turbine under several different fixed wind speeds (Table.3) were simulated. And the rotor thrust and torque obtained from the simulation (Table.4) were

compared with that obtained from the FAST simulation (Fig.3). As we can see from the curves in Fig.3 and the dates in Table.4, both the rotor thrust and torque obtained with OpenFOAM have good agreement with that obtained with FAST in case 1~7.In case 8~10, when the wind speeds are over the rated wind speed and pitch angles are set to zero, both the thrust and the torque obtained from the simulation are much stronger than those with proper pitch angles set in case 5~7. This result reminds us that how strong the force and torque can be when the wind turbine is working at a high wind speed without pitch angle.

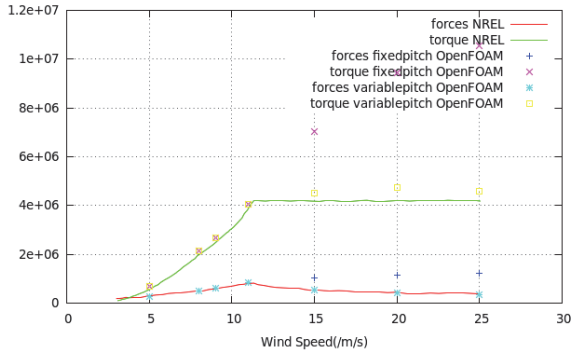

Fig 3. Rotor Thrust and Torque

Pressure Coefficient

The pressure on the surface of the blades at different wind turbines were obtained from the simulation. And the pressure coefficient can be calculated with the pressure by Eq. 2:

$$C_p = \frac{P_0 - P_\infty}{0.5\rho\left[U^2 + (\omega r)^2\right]} \quad (2)$$

In which, P_0 represents the pressure obtained from the simulation, P_∞ the pressure at infinity which is set as 0, ρ the air density, U the wind speed, ω the rotating frequency, r the rotating radius.

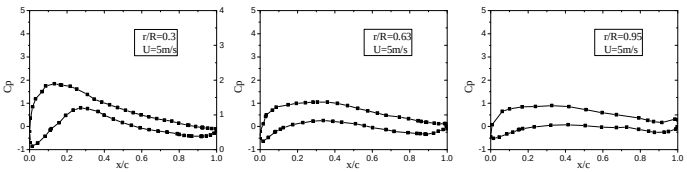

Fig 4. Pressure Coefficient under U=5 (case 1)

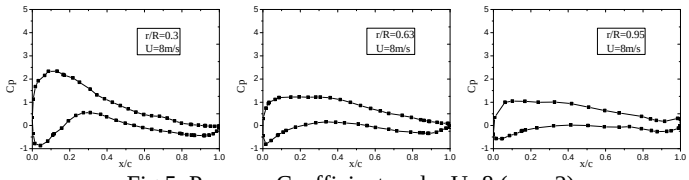

Fig 5. Pressure Coefficient under U=8 (case 2)

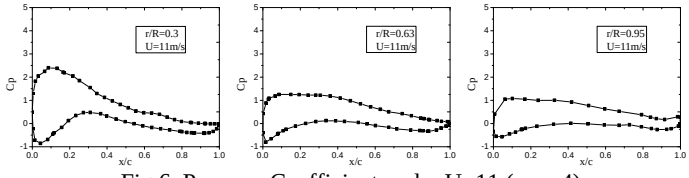

Fig 6. Pressure Coefficient under U=11 (case 4)

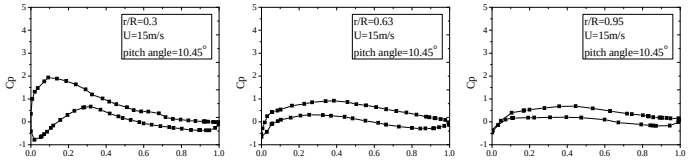

Fig 7. Pressure Coefficient under U=15 with pitch angle=10.45°(case 5)

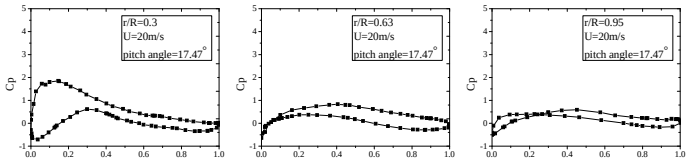

Fig 8. Pressure Coefficient under U=20 with pitch angle=17.47°(case 6)

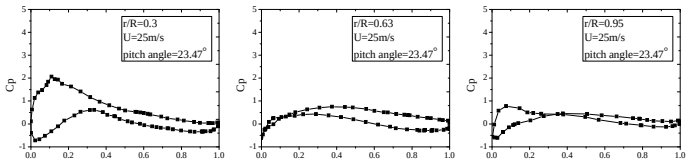

Fig 9. Pressure Coefficient under U=25 with pitch angle=23.47°(case 7)

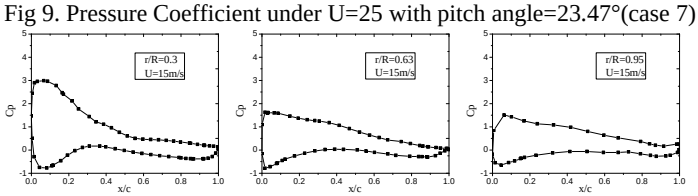

Fig 10. Pressure Coefficient under U=15 with pitch angle=0°(case 8)

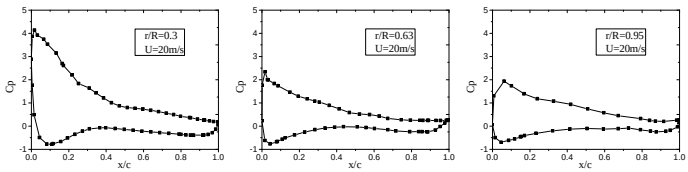

Fig 11. Pressure Coefficient under U=20 with pitch angle=0°(case 9)

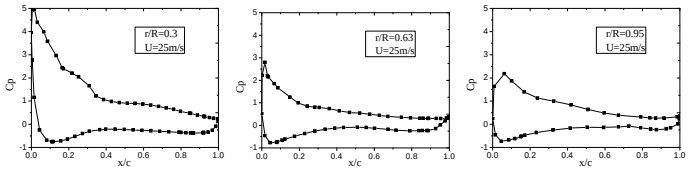

Fig 12. Pressure Coefficient under U=25 with pitch angle=0°(case 10)

In this paper, the pressure coefficient on three cross sections under six wind speeds were graphed in Figs 4~12(case 1~2,4~10). Comparing the pressure coefficient curves in three different sections of the blade, we can figure out that the pressure coefficient becomes smaller as the r/R increases from 0 to 1. Comparing the pressure coefficient curves in the same section of the blade under different wind speeds, we can conclude that the pressure coefficient grows fast as the wind speed increases with pitch angle set to zero (Fig.4~6, 10~12), especially when the wind speed increases over the rated wind speed (11.4m/s). But the pressure coefficient decreases evidently when a proper pitch angle is set (Fig.7~9). Comparing the pressure coefficient curves in Fig.7~Fig.9 to those in Fig.10~12, we can see that it's really a great challenge to the structure strength of the blade to work under wind speeds over the rated wind speed without pitch angle.

Wake Vortex

The wake vortex structure is one of the important indexes in the aerodynamic analysis of the turbine. The wake vortex near the blades has great influence on the aerodynamic properties of the blades, while the wake vortex further from the blades may influence the aerodynamic performance of other turbines behind. To get a proper wake vortex visualization result, as shown in Fig.2 (b~c), a cylindrical subdomain with the radius being 90m and a longitude of about two times of the blade radius was refined. And the second invariant of the velocity gradient tensor, Q, is used to capture the iso-surface of the vortex, which is:

$$Q = \frac{1}{2}(\Omega_{ij} \times \Omega_{ij} - S_{ij} \times S_{ij}) \quad (3)$$

In which the Ω_{ij} represents the strength of the vortex, and S_{ij} the shear strain rate.

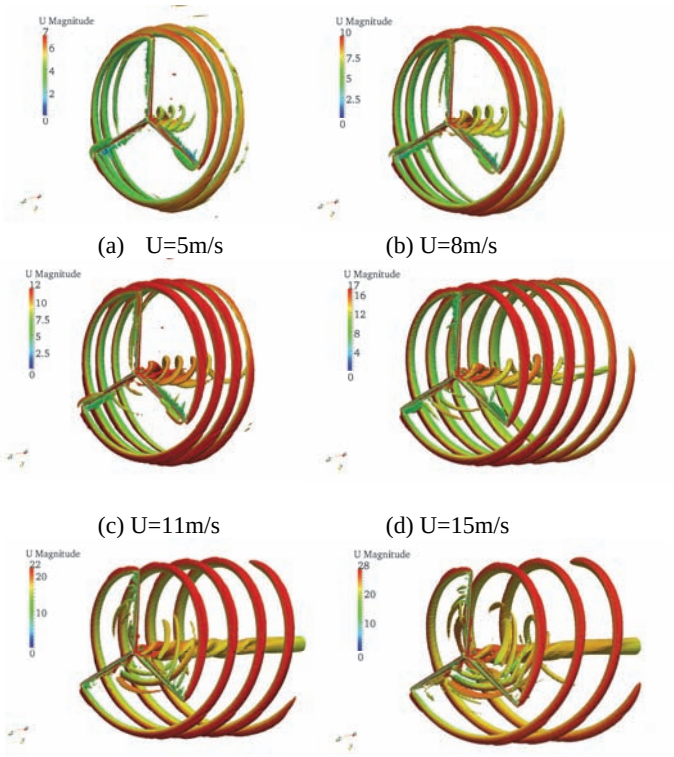

(a) U=5m/s (b) U=8m/s

(c) U=11m/s (d) U=15m/s

(e) U=20m/s (f) U=25m/s

Fig 13. The Wake Vortex

The wake vortexes at different wind speeds are listed in Fig 13. From the wake vortex structures under six fixed wind velocities listed in Fig.13, we can see that steady tip vertex and small amounts of root vortexes can be obviously observed when the wind speed is so low that the vortex shedding around the blades have not taken place yet, and that as the wind speed increases, the vortexes around the tips and the boots of the blades began to shed, and so do the ones at other part of the blades.

Limiting Streamline

As is known to all, in the viscous analysis of the flow field of the wind turbine, the velocity of the flow on the blade is equal to zero, which means no streamline exists. Limiting streamline is such a kind of streamline, of which the distance to the body surface is close but not equal to zero, so the limiting streamline actually reflects the movement of fluid micelle infinite close to the body surface. We can get more detailed information about the flow field through the limiting streamlines. The limiting streamlines on the pressure side as well as the suction side of the blade surface under three different wind speeds are shown in Fig 14.

Comparing the limiting streamlines in (a), (c) (e) and (g), we can see that limiting streamlines on the pressure side under different wind speeds show little change, while the limiting streamlines on the suction side differ a lot, with comparison of the limiting streamlines in (b), (d) (f) and (h). It is noticed that the limiting streamlines under low wind speed are so smooth that no flow separation observed, while as the wind speed increases, the flow separation occurs on the streamline of the suction side, and mainly near the trailing edge. And vortexes can be observed at high speed. Comparing limiting streamlines on the suction side in (f) and (h), more vortexes can be observed when the wind turbine works under high speed wind without pitch angle.

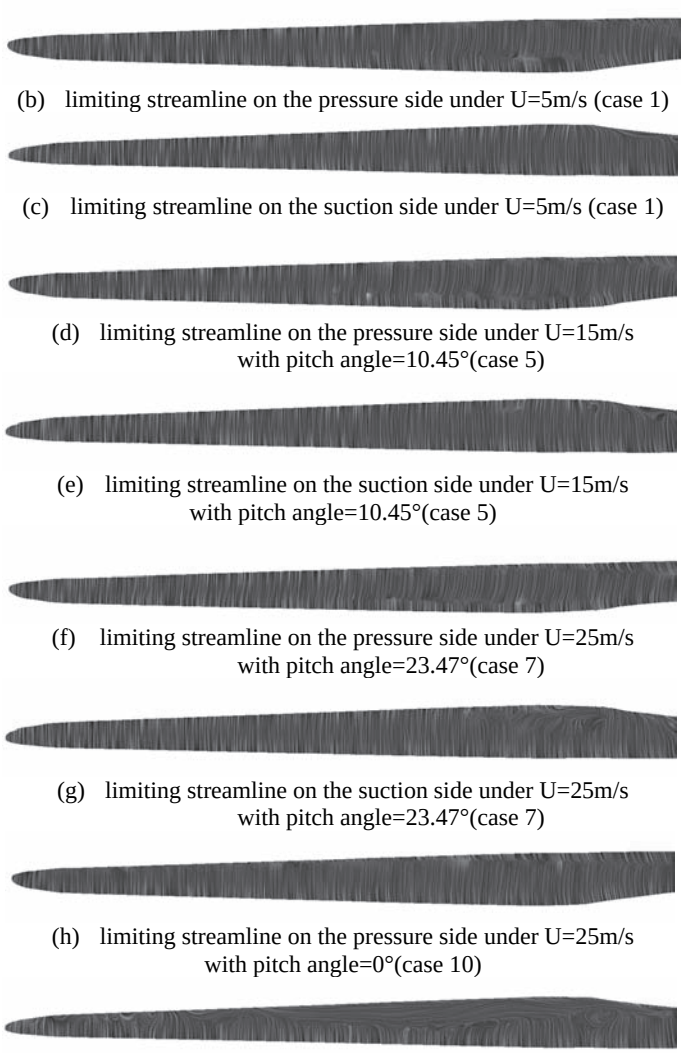

(b) limiting streamline on the pressure side under U=5m/s (case 1)

(c) limiting streamline on the suction side under U=5m/s (case 1)

(d) limiting streamline on the pressure side under U=15m/s with pitch angle=10.45°(case 5)

(e) limiting streamline on the suction side under U=15m/s with pitch angle=10.45°(case 5)

(f) limiting streamline on the pressure side under U=25m/s with pitch angle=23.47°(case 7)

(g) limiting streamline on the suction side under U=25m/s with pitch angle=23.47°(case 7)

(h) limiting streamline on the pressure side under U=25m/s with pitch angle=0°(case 10)

(i) limiting streamline on the suction side under U=25m/s with pitch angle=0°(case 10)

Fig 14. Limiting Streamline at Different Wind Speed

CONCLUSIONS

In this paper, the aerodynamic performance of the NREL offshore 5-MW baseline wind turbine under different fixed wind speeds were simulated with OpenFOAM without considering the interaction of floating structure. And the rotor thrust, torque, pressure coefficient and wake vortex aerodynamic data and flow field information were obtained in detail. One important proviso: besides seven normal cases (case 1~7), there are three cases (case 8~10) added in this paper, in which the wind speed is over the rated wind speed while the pitch angle of the turbine is set to zero.

With the rotor thrust and torque obtained from the simulation were compared with that obtained from the FAST simulation, the rotor thrust and torque obtained from the simulation in this paper show good agreement with results from the FAST simulation at normal working conditions. When the wind speeds are over the rated wind speed and pitch angles are set to zero, both the thrust and the torque obtained from the simulation are much stronger than those with proper pitch angles set.

By analyzing the pressure coefficient curves in three different sections of the blade under different wind speeds we can figure out that the pressure coefficient becomes smaller as the r/R increases from 0 to 1, and that the pressure coefficient grows fast as the wind speed increases, especially when the wind speed grows over the rated wind speed (11.4m/s). But the pressure coefficient decreases evidently when a proper pitch angle is set. And we can see that it's really a great challenge to the structure strength of the blade to work under wind speeds over the rated wind speed without pitch angle.

To get more detailed information of the turbines' aerodynamic performance, the wake vortex and the limiting streamlines were analyzed, we find that there are few vortexes under low wind speed and then the flow separation occurs as the wind speed increases.

Further work is going on, and more work can be done, such as the aerodynamic simulation of the floating wind turbine considering the interaction between the blades and the floating structure.

ACKNOWLEDGEMENTS

This work is supported by National Natural Science Foundation of China (Grant Nos. 51379125, 11272120, 51411130131), The National Key Basic Research Development Plan (973 Plan) Project of China (Grant No. 2013CB036103), High Technology of Marine Research Project of The Ministry of Industry and Information Technology of China, the Program for Professor of Special Appointment (Eastern Scholar) at Shanghai Institutions of Higher Learning (Grant No. 2013022), ABS (China) Limited and Center for HPC of Shanghai Jiao Tong University, to which the authors are most grateful.

REFERENCES

Churchfield, MJ, Lee, S, Michalakes, J, Moriarty, PJ (2012). A numerical study of the effects of atmospheric and wake turbulence on wind turbine dynamics. Journal of Turbulence, Vol 13, pp1-32.

Fleig, O, Arakawa, C (2004). Numerical simulation of wind turbine tip noise. Collection of the 2004 ASME Wind Energy Symposium Technical Papers at the 42nd AIAA Aerospace Sciences Meeting and Exhibit, pp 587-597.

Heronemus, WE (1972). Pollution-free Energy from the Offshore Winds. Marine Technology Society.

Johansen, J, Sorensen, NN, Michelsen, JA, Schreck, S (2002). Detached-eddy simulation of flow around the NREL phase-VI blade. ASME 2002 Wind Energy Symposium. American Society of Mechanical Engineers, pp 106-114.

Jonkman, JM, Buhl, Jr, ML (2007). Loads analysis of a floating offshore wind turbine using fully coupled simulation. WINDPOWER 2007 Conference and Exhibition.

Jonkman, J, Butterfield, S, Musial, W, Scott, G (2009). Definition of a 5-MW reference wind turbine for offshore system development. Golden, CO: National Renewable Energy Laboratory.

Li, Y, Paik, KJ, Xing, T, Carrica, PM (2012). Dynamic overset CFD simulations of wind turbine aerodynamics. Renewable Energy, Vol 37(1),pp 285-298.

Moriarty, PJ, Hansen, AC (2005). AeroDyn theory manual. Golden, Colorado, USA: National Renewable Energy Laboratory.

Menter, FR (1993). Zonal two equation k-ω turbulence models for aerodynamic flows.

Butterfield, CP, Musial, W, Jonkman, J, Sclavounos P (2007). Engineering challenges for floating offshore wind turbines[M]. National Renewable Energy Laboratory.

Shur M, Spalart P R, Strelets M, Travin, A (1999). Detached-eddy simulation of an airfoil at high angle of attack. Engineering turbulence modelling and experiments, pp 669-678.

Sørensen, NN, Michelsen, JA, Schreck, S (2002). Navier–Stokes predictions of the NREL phase VI rotor in the NASA Ames 80 ft× 120 ft wind tunnel. Wind Energy, Vol 5(2 3), pp 151-169.

Strelets, M (2001). Detached eddy simulation of massively separated flows. American Institute of Aeronautics & Astronautics.

Stovall, TD, Pawlas, G, Moriarty, PJ (2010). Wind farm wake simulations in OpenFOAM. AIAA Paper, pp 825.